SSIM 2021 - PM Dight (ed.)
© Australian Centre for Geomechanics, Perth, ISBN 978-0-6450938-1-0
doi:10.36487/ACG_repo/2135_05

Application of three-dimensional limit equilibrium in the slope stability assessment process

D Dwumfour *Fortescue Metals Group, Australia*

J Dixon *Fortescue Metals Group, Australia*

P Croft *Brockman Solutions, Australia*

M Fredlund *Bentley Systems, Canada*

Abstract

The utilisation of three-dimensional limit equilibrium in evaluating open pit slope stability is becoming increasingly common in the industry. Implementation of this assessment approach requires developing new assessment workflows associated with the model inputs to ensure confidence in the modelling outcomes and leveraging the full benefits of the approach. Several challenges also exist in terms of understanding data reliability and software capability; a particular limitation identified was the practical application of the disturbance zone behind the slope. This paper provides a workflow adopted to ensure high confidence in the modelling outcomes and communication of the assessment results using a case study and highlights the software developments to address limitations.

Keywords: *geotechnical, slope stability analysis*

1 Introduction

The use of three-dimensional (3D) limit equilibrium geotechnical software packages in slope stability analysis is becoming increasingly common as part of the geotechnical slope assessment process. There can be significant benefits in using 3D software application in the slope assessment process flow, especially for slopes of moderate or high consequence of failure. Some of the benefits are:

- Improved confidence in the design.
- Maximising slope design optimisation potential and hence, ore recovery.
- Informing the slope monitoring strategy and planning.
- Unexpected critical areas may be exposed with spatial searching.
- A higher Factor of Safety (FoS) compared to the results from the two-dimensional (2D) assessment is obtained the majority of times.
- 3D analysis offers improvements in evaluating the impact of the selected mining method compared to a 2D assessment package.

The above benefits can only be realised if the input parameters of the modelling have a reasonable to high (acceptable level of) confidence as the reliability of the stability assessment depends on input parameters. High confidence is also required for the topography, the geological surface/s, and the porewater pressures/groundwater data, if applicable.

This paper provides a workflow that Fortescue has adopted in the 3D modelling process to ensure that reasonable confidence is achieved in calculating the FoS of pit slopes. A case study of 3D modelling using the workflow for one of the pits within the Western Hub mine is provided.

2 3D modelling process flow

The following are the required input models in the form of 3D wireframes or distinct input values for 3D limit equilibrium modelling of a mine pit as outlined in the slope design process (Read & Stacey 2009):

- Pit design.
- Structural/geological surface/s from the geological models.
- Hydrogeology model surface (groundwater drawdown surface), if applicable.
- Geotechnical shear strength for the applicable model domains (the rock mass model).

To ensure the required level of reliability is achieved for the assessment, it is vital that all the necessary inputs for the model have a commensurate level of confidence and that the user understands the limitations well. The derivation of geotechnical parameters and recommended confidence are provided in industry guidelines such as Read & Stacey (2009).

The 3D model output is significantly impacted by the geological surfaces intersected by trial slip surfaces evaluated by the slope stability software. These surfaces should have a level of confidence that is acceptable to the design risk. The level of confidence is related to the space between drill holes and the interpolation method utilised. Limitations on the geological surface should also be documented.

The typical workflow for any 2D slope stability assessment is presented below:

- Slope configuration validation as per design report.
- Selection of critical section based on depth, unfavourable structures, weak geological unit, groundwater drawdown, bullnose, or critical infrastructure close to the pit after completion of slope configuration validation.
- Detailed slope stability of critical sections using the 2D geotechnical package for the FoS and evaluate results against design acceptance criteria.

The challenge with the process outlined above is that it is possible that the critical section of the slope may be overlooked. This can especially be true where the slope designer has limited design experience or by an oversight.

A 3D assessment using PLAXIS 3D LE (Bentley Systems 2021) follows a similar process flow as the 2D workflow. The primary difference is that after the slope configuration validation, the modelling workflow changes such that the 3D model is built from the pit design and verified geological surfaces in the geotechnical slope stability software. Once the model is built, the 3D model package uses the multiplane analysis (MPA) feature that provides an option to have sections to cover the entire pit slope geometry area as part of the initial design stability check (Figure 1). This approach increases the potential for all critical slopes to be identified and captured in the initial assessment. For the initial assessment, a much coarser column spacing is used to ensure a reduced computation time. With the PLAXIS 3D LE package, both 2D and 3D assessment can be undertaken for the same sections using the MPA option. This allows a detailed evaluation of the 2D and 3D analysis results at the same section as part of the pit design evaluation. The results from the initial assessment are then evaluated, and critical areas of the slope noted. A final assessment is undertaken at the identified critical areas of the slope using a high mesh density. The computation time is typically longer, and results are much more refined compared to the initial assessment.

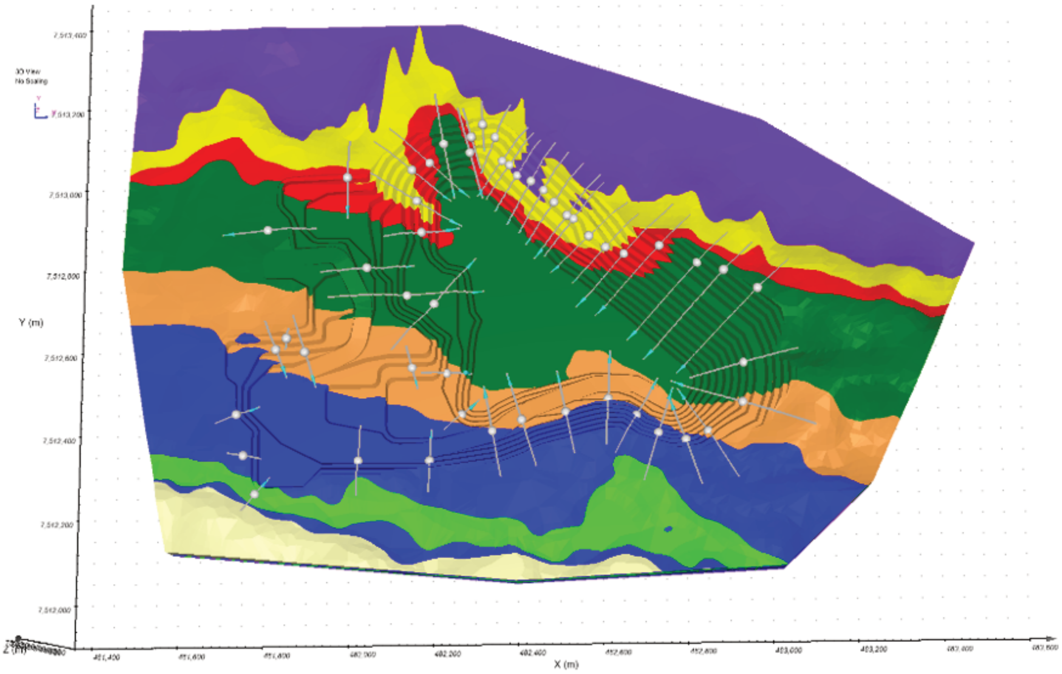

Figure 1 Plan view of sections for the 3D model using the multiplane analysis from PLAXIS 3D LE

The adopted 3D stability assessment process flow is presented below:

- Slope configuration validation as per design report.
- Construction of a 3D model of the pit using the validated design and available geological and hydrogeological surface.
- Selection of sections to cover entire pit design based on depth, unfavourable structures, weak geological units, groundwater drawdown, bullnose or existence of critical infrastructure if applicable.
- Running of a 2D and 3D MPA on the selected sections using a lower column resolution.
- Evaluate both 2D and 3D results for critical areas within the pit design.
- Re-run a 3D multiplane assessment of the critical areas with a higher mesh density.

The reliability and confidence of the results of the 3D model assessment are dependent on all the input parameters, especially the geological surfaces used in building the model. The process adopted in ensuring the confidence and risk of the geological surfaces is communicated to all stakeholders as presented in Section 3. This process follows a similar approach developed by Savage et al. (2013).

3 Geological model

The geological model, represented by surfaces, is among the important input parameters required to evaluate the slope stability of the pit. A 3D geotechnical stability assessment of a slope is sensitive to variations in the geological interpretation where the trial slip surfaces pass through the geological structures such as the bedded units within the Pilbara; hence, any degree of variability inherent in the interpretation must be communicated to the pit designer.

The geological interpretation can be based on a wide range of data types and data densities. The geological wireframe surfaces generated from the interpretation can sit on a reliability spectrum ranging from conceptual (derived from minimal data points) through to high confidence wireframes derived from multiple data sources containing hundreds of reliable data points. Geological confidence data is a way to display the variability in the confidence of the interpretation. It is derived from the quantity and quality of the data that has been used to interpret a geological feature. The geological feature may represent a stratigraphic horizon, lithological contact, or significant fault or joint.

When using Vulcan software (Maptek 2021), the confidence data is stored in a layer used in conjunction with a corresponding wireframe surface of a geological feature. Within the Vulcan layer are 'W' tagged points that relate to the location of a piece of data (drillhole intercept, mapped shale band, etc.) utilised to interpret the feature. Each point is assigned a colour-coded confidence rating ranging in value from 1 (very high confidence +/- <2 m data accuracy) to 5 (very low confidence +/- >20 m data accuracy). This rating is an estimate of the level of spatial accuracy of the data point. The ratings and assigned levels of accuracy are displayed in Table 1.

Table 1 Confidence ratings

Rating	Confidence level	Data accuracy	Colour
1	Very high	+/- <2 m	🟦
2	High	+/- 2–5 m	🟩
3	Moderate	+/- 5–10 m	🟨
4	Low	+/- 10–20 m	🟧
5	Very low	+/- >20 m	🟥

3.1 Data types and degrees of confidence

All data types can have varying degrees of confidence depending on the level of spatial accuracy of the data. The following are examples of commonly used data sets and their calculated degrees of confidence.

3.1.1 Drilling gamma logs

The geological interpretation is commonly completed by identifying the distinctive stratigraphic signatures within the geophysical gamma logs. When the drillhole location has been accurately recorded, i.e. the drill collar has been surveyed, and the hole has completed downhole survey from either gyro or magnetic survey tool, then provided there is a consistent and identifiable gamma signature, a high level of confidence (W tag = 1) can be assigned to the confidence data points. Figure 2 is an illustration of a very high confidence data point.

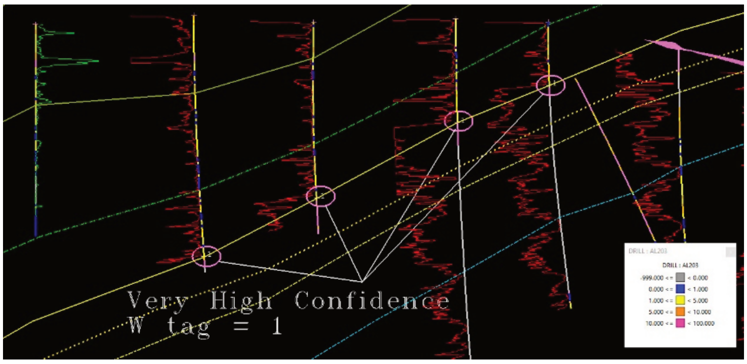

Figure 2 Very high confidence (W tag 1, accurate to 2 m) data points assigned to reliable gamma signature from surveyed drill holes

3.1.2 Gamma logs: inferred

Confidence data can be inferred from an adjacent boundary when no gamma data is present. The inferred confidence data is downgraded one level to reflect the reduced level of spatial accuracy. Figure 3 is a typical illustration of the inferred surface.

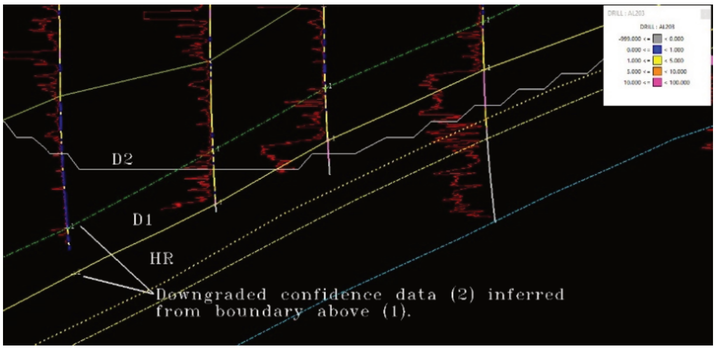

Figure 3 Inferred confidence data

Geological features such as faults are commonly interpreted from stratigraphic offsets between adjacent drill holes and, as a result, can have lower confidence ratings to reflect the larger degree of uncertainty in the interpretation, as shown in Figure 4.

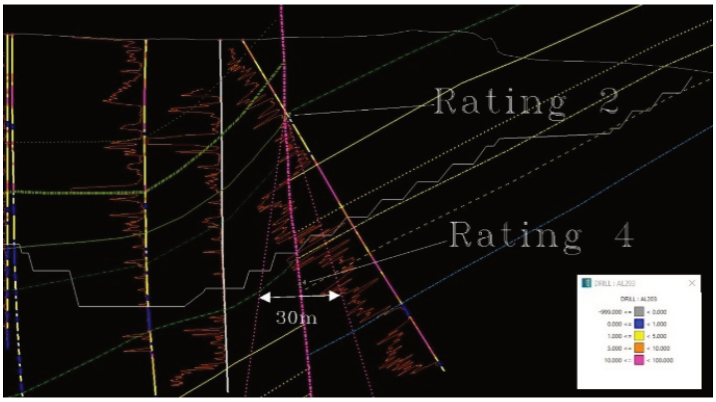

Figure 4 Cross-section fault interpretation, stratigraphic offset between adjacent drill holes: rating 4

3.1.3 Drilling: no downhole survey

Drilling with no downhole survey can introduce significant errors into the geological model. If an interpretation includes drilling with little or no downhole survey, this needs to be reflected in the confidence data assigned to the points related to those drill holes. Vertical holes containing downhole survey can be used to calculate ranges of confidence which can be assigned to the holes with no downhole survey. Figure 5 displays the drilling for a mining deposit within the Pilbara, where only the vertical holes containing downhole survey data have been loaded, and the holes are colour-coded by depth. The vertical distance variation for each depth interval was measured, and the results are tabulated in Table 2. From this, an estimate can be made of the deviation of a vertical hole with depth. In this example, 21 holes were measured at 200 m depth, and their horizontal variance from the drill collar were noted to range from 6 m to 39 m with an average of 17.0 m. The average values in Table 2 are then applied as confidence data W tag values in the interpretation at a given depth where drill holes have no downhole survey. This is illustrated in Figure 6. Non vertical drill holes are treated in a similar manner.

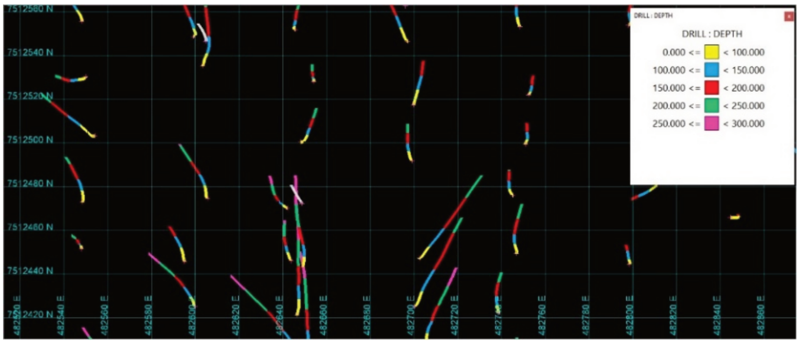

Figure 5 **Vertical drillholes with downhole survey used to measure the horizontal variance from drill collar to depth interval**

Table 2 **Measured horizontal variance for given depths: assigned confidence rating**

Depth (m)	Range (m)	Number	Average variance (m)	Rating
100	1–9	36	5	3
150	2–20	36	10	4
200	6–39	21	17	4
250	13–45	14	27	5

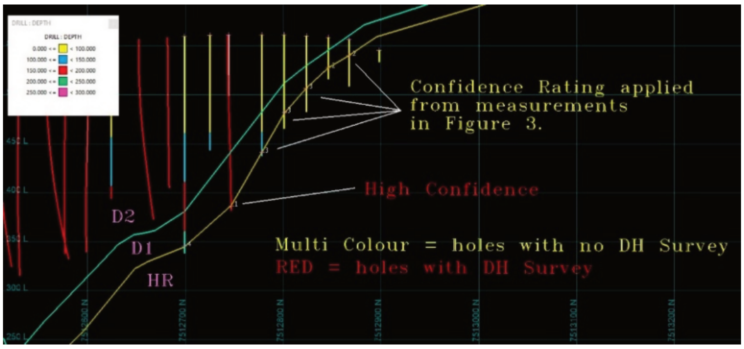

Confidence Rating applied from measurements in Figure 3.

High Confidence

Multi Colour = holes with no DH Survey
RED = holes with DH Survey

Figure 6 **Calculated confidence levels assigned to drill holes with no downhole survey**

3.1.4 Drilling geochemistry

Drilling that contains composited (2–3 m interval) distinctive geochemistry can be used to assign confidence data to the interpretation. The confidence levels should be downgraded to reflect the width of the composited interval. Additionally, an inferred stratigraphic boundary adjacent to a rating 1 boundary can be assigned a downgraded rating of 2, as shown in Figure 7.

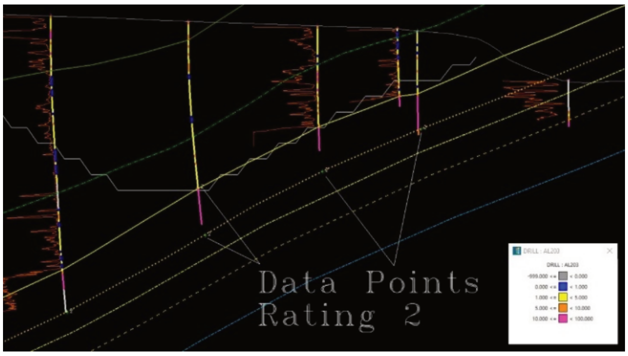

Data Points Rating 2

Figure 7 **Cross-section interpretation utilising distinctive geochemistry and inferred adjacent stratigraphy: rating 2**

3.1.5 Mapping

When used in an interpretation, face mapping and surface mapping data can be assigned confidence ratings. The confidence ratings will generally reflect the degree of survey control used in the mapping for face mapping. For example, geological features digitised on high-resolution georeferenced imagery will have an accuracy of +/- <2 m and can be assigned a confidence rating of 1, as shown in Figure 8. Whereas face mapping conducted using 30 m spaced surveyed reference points will have an accuracy of +/- 2–5 m and can be assigned a confidence rating of 2. Geological contacts mapped during surface mapping are commonly observed to have an accuracy of +/- 5–10 m and are assigned a confidence rating of 3.

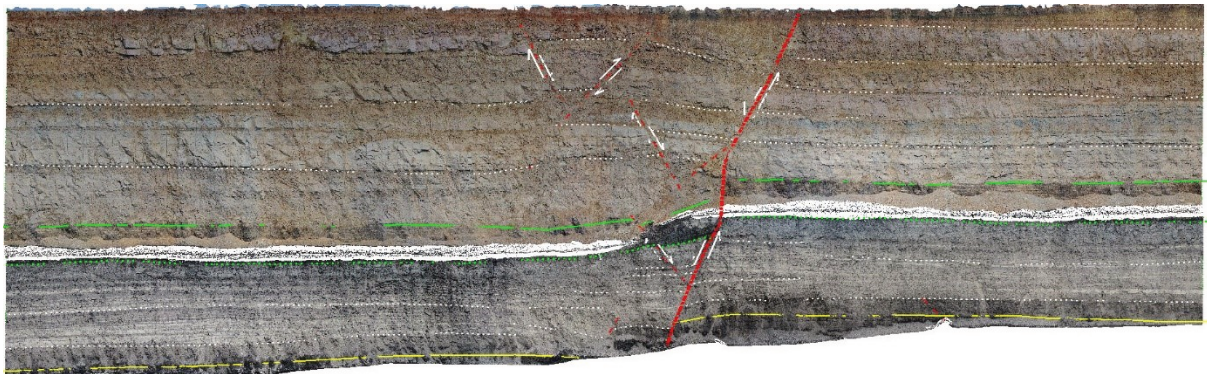

Figure 8 Fault digitised on a high-resolution georeferenced image: confidence rating 1

Once the confidence data has been assigned to the various data sets used in the interpretation, the Vulcan layer and the 'W' tagged confidence data points can be viewed with the corresponding wireframe surface. This data can then be used in the geotechnical design process. Figure 9 shows a structurally verified geological surface showing a confidence rating for the data points.

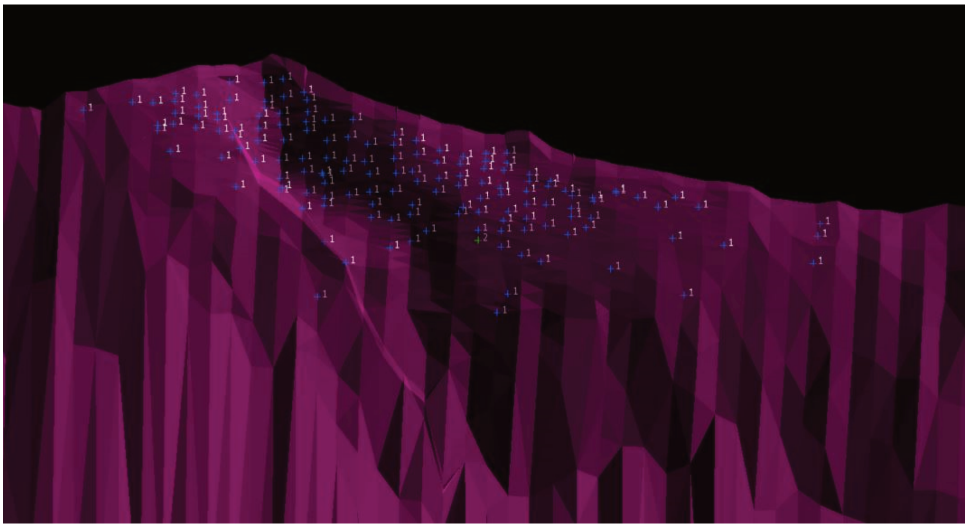

Figure 9 Wireframe showing its confidence data

4 Case study

The above process flow and the geological surfaces assessed for confidence were adopted to evaluate the slope stability of a staged pit design within the Pilbara region of Western Australia.

4.1 Pit design

The stage pit design, Figure 10, was designed to be above the groundwater table.

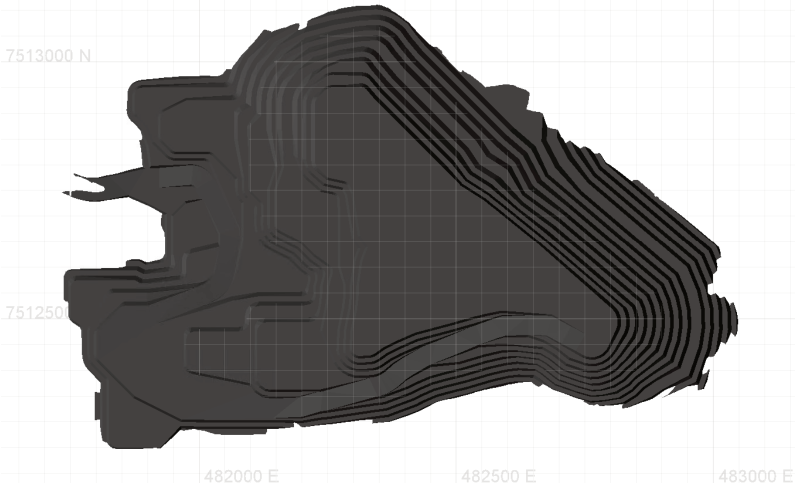

Figure 10 Plan view of the case study pit design

4.2 Geology

The mining area is within the southern limb of the east–west trending Jeerinah Anticline in the western part of the Hamersley Range. Mineralisation in the project area occurs in the Brockman iron formation. It is typically (though not always) located within second-order synclines in the limbs of the anticline. Mineralisation in the Brockman iron formation is predominantly found within the Joffre and Dales Gorge Members. Mineralisation in the Marra Mamba banded iron formation units is confined largely to the Mount Newman and MacLeod Members. Figure 11 shows the geology within the West End Area.

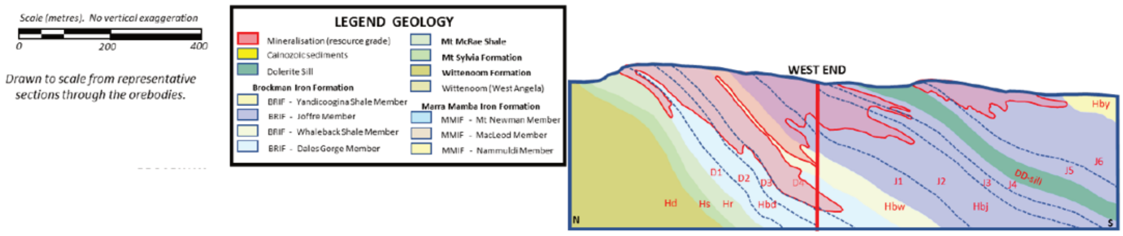

Figure 11 Typical strata of the Western Hub project (West End) area facing west (Simpson & Walker 2019)

Cainozoic and Quaternary detrital materials overlie the weathered shales of the Wittenoom formation and Mount McRae Shale locally to depths of up to 50 m.

4.3 Geotechnical assessment review

The review focused on the 2D and 3D slope stability assessment using PLAXIS 3D LE and combines the following to compute the FoS:

- The overall height of the pit slope in each sector.
- The geological properties that may impact the stability of the pit slope, e.g. weaker geological units or steeply dipping bedding planes.
- The pit design shape such as any bullnoses or confinement.

The design slope stability models were compiled using the geological model surfaces with defined data confidence levels as described in Section 3. PLAXIS 3D LE slope stability software was utilised for the assessment. The linear anisotropic shear strength function developed during the feasibility studies (Red Rock Geotechnical 2019) was adopted as the material shear strength parameter.

4.4 Geotechnical acceptance criteria

Except for the northwestern section of Stage 2, which forms part of the ultimate pit, all other walls are interim. A landbridge exists north of the pit. Based on Fortescue internal risk assessment using the above information, a 'low to moderate consequence' of failure was adopted for this pit design. Design acceptance criteria in alignment with the guidelines on slope stability were adopted.

4.5 Slope configuration

The pit minimum berm width, batter height, and the batter face angle were assessed to conform to the recommended slope design configuration parameters (Figure 12).

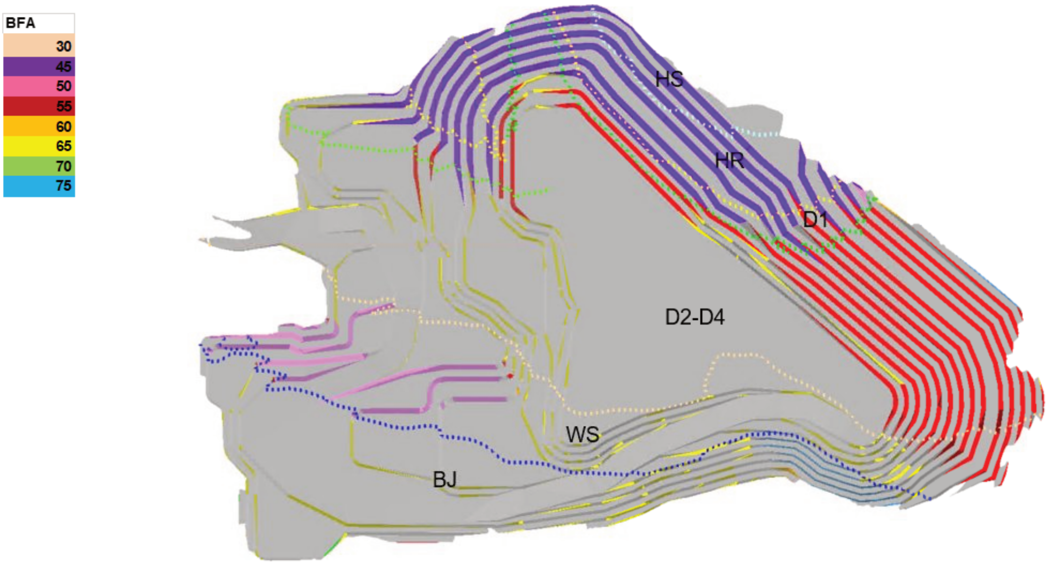

Figure 12 Batter face configuration checks

4.6 Stability assessment

For the stability assessment, the following scenarios were evaluated:

- A 3D assessment with its corresponding 2D assessment without any minimum slide surface depth filter is used to evaluate the batter scale and multi bench scale.
- A 3D assessment with its corresponding 2D assessment with a minimum slide surface depth based on the batter to berm configuration of the slope to obtain the inter-ramp/overall slope stability.

Figures 13 and 14 present the FoS contours for the initial assessment where minimum slide surface depth equivalent to the berm width was applied to obtain the inter-ramp/overall slope FoS. Figure 15 is the overall FoS contour for the critical area (northeast) as assessed from the previous assessment using a higher mesh density of 600 column (slices) and 600 rows.

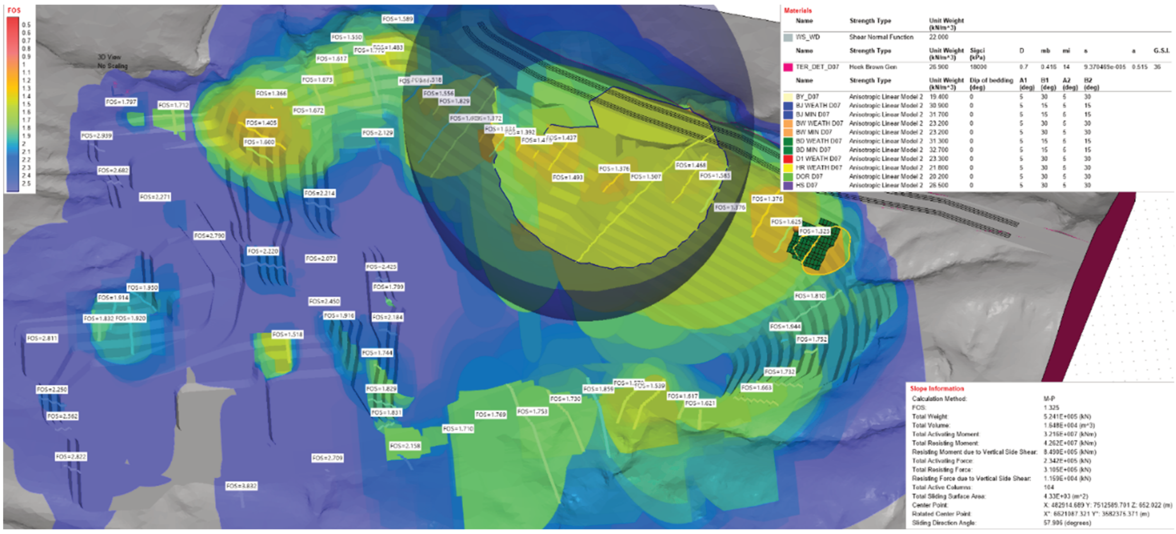

Materials

	Name	Strength Type	Unit Weight (kN/m^3)							
▨	WS_WD	Shear Normal Function	22.000							
	Name	**Strength Type**	**Unit Weight (kN/m^3)**	**Sigci (kPa)**	**D**	**mb**	**mi**	**s**	**a**	**G.S.I.**
🟥	TER_DET_D07	Hoek Brown Gen	26.900	18000	0.7	0.416	14	9.370469e-005	0.515	36
	Name	**Strength Type**	**Unit Weight (kN/m^3)**	**Dip of bedding (deg)**	**A1 (deg)**	**B1 (deg)**	**A2 (deg)**	**B2 (deg)**		
▨	BY_D07	Anisotropic Linear Model 2	19.400	0	5	30	5	30		
🟦	BJ WEATH D07	Anisotropic Linear Model 2	30.900	0	5	15	5	15		
🟦	BJ MIN D07	Anisotropic Linear Model 2	31.700	0	5	15	5	15		
🟧	BW WEATH D07	Anisotropic Linear Model 2	23.200	0	5	30	5	30		
🟧	BW MIN D07	Anisotropic Linear Model 2	23.200	0	5	30	5	30		
🟩	BD WEATH D07	Anisotropic Linear Model 2	31.300	0	5	15	5	15		
🟩	BD MIN D07	Anisotropic Linear Model 2	32.700	0	5	15	5	15		
🟥	D1 WEATH D07	Anisotropic Linear Model 2	23.300	0	5	30	5	30		
🟨	HR WEATH D07	Anisotropic Linear Model 2	21.800	0	5	30	5	30		
🟩	DOR D07	Anisotropic Linear Model 2	20.200	0	5	30	5	30		
🟪	HS D07	Anisotropic Linear Model 2	26.500	0	5	30	5	30		

Slope Information

Calculation Method:	M-P
FOS:	1.325
Total Weight:	5.241E+005 (kN)
Total Volume:	1.648E+004 (m^3)
Total Activating Moment:	3.216E+007 (kNm)
Total Resisting Moment:	4.262E+007 (kNm)
Resisting Moment due to Vertical Side Shear:	8.490E+005 (kNm)
Total Activating Force:	2.342E+005 (kN)
Total Resisting Force:	3.105E+005 (kN)
Resisting Force due to Vertical Side Shear:	1.159E+004 (kN)
Total Active Columns:	104
Total Sliding Surface Area:	4.33E+03 (m^2)
Center Point:	X: 482914.689 Y: 7512589.701 Z: 652.022 (m)
Rotated Center Point:	X*: 6621087.321 Y*: 3682376.371 (m)
Sliding Direction Angle:	57.906 (degrees)

Figure 13 The Factor of Safety contour for the 3D inter-ramp/overall scale assessment

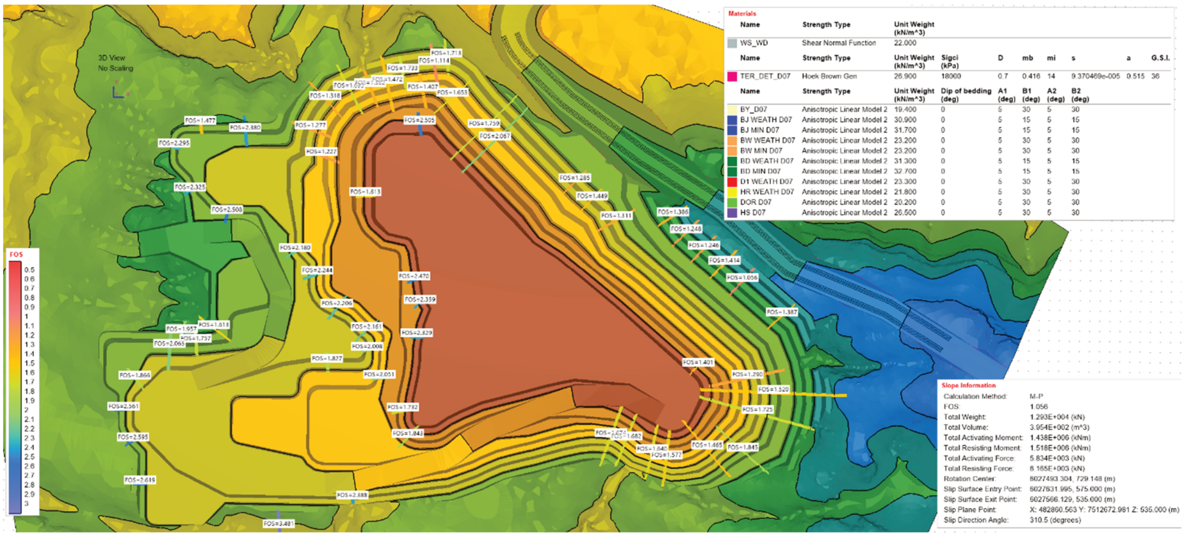

Materials

	Name	Strength Type	Unit Weight (kN/m^3)							
▨	WS_WD	Shear Normal Function	22.000							
	Name	**Strength Type**	**Unit Weight (kN/m^3)**	**Sigci (kPa)**	**D**	**mb**	**mi**	**s**	**a**	**G.S.I.**
🟥	TER_DET_D07	Hoek Brown Gen	26.900	18000	0.7	0.416	14	9.370469e-005	0.515	36
	Name	**Strength Type**	**Unit Weight (kN/m^3)**	**Dip of bedding (deg)**	**A1 (deg)**	**B1 (deg)**	**A2 (deg)**	**B2 (deg)**		
▨	BY_D07	Anisotropic Linear Model 2	19.400	0	5	30	5	30		
🟦	BJ WEATH D07	Anisotropic Linear Model 2	30.900	0	5	15	5	15		
🟦	BJ MIN D07	Anisotropic Linear Model 2	31.700	0	5	15	5	15		
🟧	BW WEATH D07	Anisotropic Linear Model 2	23.200	0	5	30	5	30		
🟧	BW MIN D07	Anisotropic Linear Model 2	23.200	0	5	30	5	30		
🟩	BD WEATH D07	Anisotropic Linear Model 2	31.300	0	5	15	5	15		
🟩	BD MIN D07	Anisotropic Linear Model 2	32.700	0	5	15	5	15		
🟥	D1 WEATH D07	Anisotropic Linear Model 2	23.300	0	5	30	5	30		
🟨	HR WEATH D07	Anisotropic Linear Model 2	21.800	0	5	30	5	30		
🟩	DOR D07	Anisotropic Linear Model 2	20.200	0	5	30	5	30		
🟪	HS D07	Anisotropic Linear Model 2	26.500	0	5	30	5	30		

Slope Information

Calculation Method:	M-P
FOS:	1.056
Total Weight:	1.293E+004 (kN)
Total Volume:	3.954E+002 (m^3)
Total Activating Moment:	1.438E+006 (kNm)
Total Resisting Moment:	1.518E+006 (kNm)
Total Activating Force:	5.834E+003 (kN)
Total Resisting Force:	6.165E+003 (kN)
Rotation Center:	6027493.304, 729.148 (m)
Slip Surface Entry Point:	6027631.995, 575.000 (m)
Slip Surface Exit Point:	6027566.129, 535.000 (m)
Slip Plane Point:	X: 482860.563 Y: 7512672.981 Z: 535.000 (m)
Slip Direction Angle:	310.5 (degrees)

Figure 14 2D inter-ramp/overall Factor of Safety for the same section location as the 3D in Figure 13

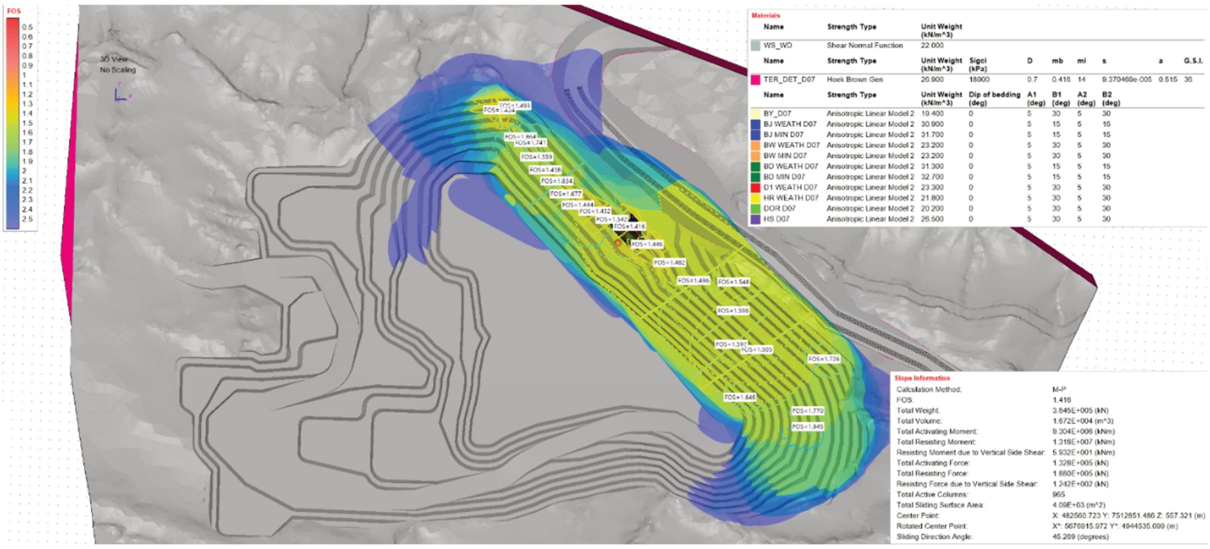

Materials

	Name	Strength Type	Unit Weight (kN/m^3)							
▨	WS_WD	Shear Normal Function	22.000							
	Name	**Strength Type**	**Unit Weight (kN/m^3)**	**Sigci (kPa)**	**D**	**mb**	**mi**	**s**	**a**	**G.S.I.**
🟥	TER_DET_D07	Hoek Brown Gen	26.900	18000	0.7	0.416	14	9.370469e-005	0.515	36
	Name	**Strength Type**	**Unit Weight (kN/m^3)**	**Dip of bedding (deg)**	**A1 (deg)**	**B1 (deg)**	**A2 (deg)**	**B2 (deg)**		
▨	BY_D07	Anisotropic Linear Model 2	19.400	0	5	30	5	30		
🟦	BJ WEATH D07	Anisotropic Linear Model 2	30.900	0	5	15	5	15		
🟦	BJ MIN D07	Anisotropic Linear Model 2	31.700	0	5	15	5	15		
🟧	BW WEATH D07	Anisotropic Linear Model 2	23.200	0	5	30	5	30		
🟧	BW MIN D07	Anisotropic Linear Model 2	23.200	0	5	30	5	30		
🟩	BD WEATH D07	Anisotropic Linear Model 2	31.300	0	5	15	5	15		
🟩	BD MIN D07	Anisotropic Linear Model 2	32.700	0	5	15	5	15		
🟥	D1 WEATH D07	Anisotropic Linear Model 2	23.300	0	5	30	5	30		
🟨	HR WEATH D07	Anisotropic Linear Model 2	21.800	0	5	30	5	30		
🟩	DOR D07	Anisotropic Linear Model 2	20.200	0	5	30	5	30		
🟪	HS D07	Anisotropic Linear Model 2	26.500	0	5	30	5	30		

Slope Information

Calculation Method:	M-P
FOS:	1.416
Total Weight:	3.645E+005 (kN)
Total Volume:	1.672E+004 (m^3)
Total Activating Moment:	9.304E+006 (kNm)
Total Resisting Moment:	1.318E+007 (kNm)
Resisting Moment due to Vertical Side Shear:	5.932E+001 (kNm)
Total Activating Force:	1.328E+005 (kN)
Total Resisting Force:	1.880E+005 (kN)
Resisting Force due to Vertical Side Shear:	1.242E+002 (kN)
Total Active Columns:	965
Total Sliding Surface Area:	4.09E+03 (m^2)
Center Point:	X: 482560.723 Y: 7512851.486 Z: 557.321 (m)
Rotated Center Point:	X*: 5676915.972 Y*: 4944535.099 (m)
Sliding Direction Angle:	45.269 (degrees)

Figure 15 3D overall Factor of Safety for high-density mesh for northeastern wall (critical area)

A summary of the inter-ramp and overall results from the 2D and 3D (lower and higher density) are presented in Table 3.

Table 3 Summary of the Factor of Safety

Minimum Factor of Safety	2D assessment	3D assessment (lower density mesh)	3D assessment (higher density mesh)	Comments
Inter-ramp	1.05	1.33	1.42	The 3D results were all at same location on the northeastern wall
Overall	1.52	1.51	1.50	

4.7 Discussion of assessment results

The section with the minimum FoS in 2D returned an FoS of 1.05 (the 3D FoS at the same location from the initial 3D assessment is 1.37). The 3D assessment using a lower mesh density or resolution returned a minimum FoS of 1.33. Its 2D corresponding FoS is 1.39; the lower FoS in 3D was due to the geometry of the pit slope and model resolution.

The results from the higher mesh density (Figure 15) resulted in a slightly lower overall 3D FoS of 1.50 compared to the initial assessment of about 1.51. A higher minimum inter-ramp FoS of 1.42 was also obtained at a different location (further east) compared to the FoS of 1.33 from the initial 3D assessment (the final FoS at this location based on the higher density is 1.73). To obtain the final 3D results, especially for very critical sections, it is important to always run the model at a higher resolution to check if the FoS significantly changes. It is also important to ensure that the geological surfaces have been assessed for confidence level before using any 3D assessment to understand design risk and ensure reliable assessment results.

The batter scale 3D assessment results indicated the potential for shallow batter scale instability to occur and helps inform slope stability monitoring and implementation of operational controls as part of the slope risk management process.

If the geological surfaces from which the 3D slope stability model has been derived have an acceptable level of confidence (such as high to very high) and there are no artificially created surface roughness or lock-in structures, then the results from the 3D assessment are expected to have a high confidence level. This is due, in part, to the fact that most slope failures are 3D in nature. FoS calculated results from such 3D assessment are favoured over the 2D assessment results due to the 3D model being more closely aligned with reality.

5 Challenges in the 3D package usage

The primary limitation initially realised with creating the 3D model during the evaluation period was the application of both the disturbed and undisturbed zones within a 3D model. Such creation of blasting disturbance zones can be done in any 2D geotechnical package as per the Hoek (2012) recommendation on blast damage factor.

The software developers have since implemented a code within the package to apply both the blast disturbed and undisturbed zones for models that use the Generalised Hoek shear strength parameters. A code to enable models that adopt the linear anisotropic shear strength model, such as the shear-normal function, to implement both disturbed and undisturbed zone within the same model is understood to be currently under development.

Currently, models are initially built having disturbance on the entire slope as a conservative assessment. If the design meets the design acceptance criteria (DAC), no further assessment is undertaken. For models that resulted in marginal FoS compared to the DAC, an additional model is run with no disturbance. As the actual answer lies between the two 3D results, the two results may be used in evaluating the risk of slope failure for the pit. To aid with this assessment, a typical 2D assessment of the critical slope with both disturbed and undisturbed zone is used to complement the results.

6 Conclusion

The above process flow for 3D limit equilibrium geotechnical modelling is still being refined and improved as more complex designs are evaluated using the PLAXIS 3D LE package. Since the adoption of the package in the design process, the following benefits have been realised.

- Improved confidence in design stability results.
- Once the initial model has been built, the analysis time for design revision assessments reduces significantly.
- The results from the 3D analysis have facilitated increased confidence in quantifying risk.

References

Bentley Systems 2021, *PLAXIS 3D LE*, version 21.02.00.170, Bentley Systems, Exton, https://www.bentley.com/en/products/product-line/geotechnical-engineering-software/plaxis-le

Hoek, E 2012, 'Blast Damage Factor D', *RocNews*, Winter 2012 issue.

Maptek 2021, *Vulcan*, version 2021.2, Maptek Pty Ltd, Glenside, https://www.maptek.com/products/vulcan/

Read, J & Stacey, P 2009, *Guidelines for Open Pit Slope Design*, CSIRO Publishing, Clayton.

Red Rock Geotechnical Pty Ltd 2019, *WH-RP-GE-0005 Western Hub FS update-West End Pit*, geotechnical design report.

Savage N, Nicholas L, Wilson A & Seery J 2013, 'Visual communication of geological confidence - a move towards a less subjective approach', *Proceedings of Iron Ore Conference 2013*, Australasian Institute of Mining and Metallurgy, Carlton, pp. 169–173.

Simpson, C & Walker, R 2019, 'Eliwana iron ore deposits', *Proceedings of Iron Ore Conference 2013*, Australasian Institute of Mining and Metallurgy, Carlton, pp. 509–519.